Supporting Information

Charge Dispersion and Its Effects on Reactivity of Thiamin-Derived Breslow Intermediates

Michael Bielecki, Graeme W. Howe, and Ronald Kluger*

Davenport Chemistry laboratories, Department of Chemistry, University of Toronto, Toronto, Ontario M5S 3H6 Canada

*E-mail: r.kluger@utoronto.ca

Contents

Synthesis

General Considerations

Commercially available acetophenones were oxidizes to the corresponding benzoylformic acids based on a previously reported procedure where selenium dioxide is used as an oxidant and pyridine as solvent.[1] The methyl esters were prepared by methylation with dimethyl sulfate, and *tert*-butyl esters were obtained by an acid catalyzed reaction with liquid isobutylene; both procedures are described below. Finally, the *para*- and *meta*-substituted mandelylthiamin derivatives were synthesized by condensing the benzoylformate esters with *O*-TBDP-protected thiamin chloride, followed by hydrolysis to the desired product according to a method previously described by us.[2]

Overall synthesis scheme:

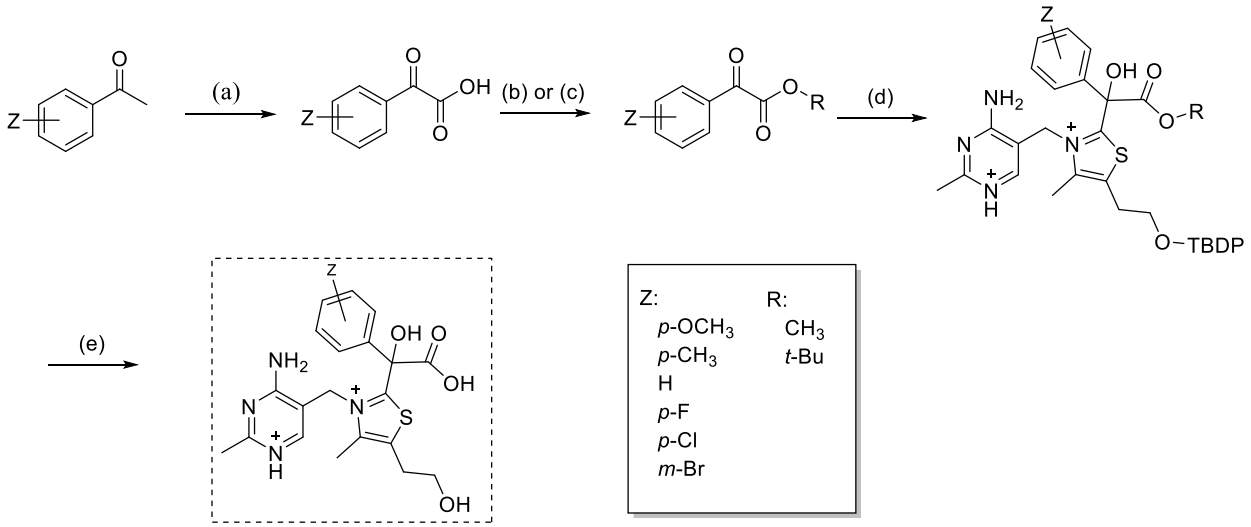

Scheme S1. Synthetic steps leading to formation of MTh and its *p*- and *m*-derivatives.

Reagents/Conditions: (a) i. SeO_2 2 eq, pyridine, reflux, overnight; ii. extraction (b) i. Me_2SO_4 1.5 eq, K_2CO_3 2 eq, DMSO, 25 ^oC, 20 min; ii. extraction (c) i. isobutylene in DCM, 25 ^oC, 24 h ii. NH_3 quench iii. extraction (d) i. O-TBDP-thiamin chloride 0.20 eq, 1M LiHMDS in toluene 0.3 eq, DCM, -20 ^oC, 5 min; ii. AcOH+TFA quench; iii. NaBr-impregnated silica flash chromatography (d) i. 36% HCl, 25 ^oC, 1-4 days; ii. extraction with DCM.

General procedure for preparation of methyl benzoylformates

5.00 mmol of a benzoylfomic acid was combined with potassium carbonate (1.00 g, 1.70 mmol) in 2.0 mL of DMSO. Dimethyl sulfate (0.57 mL, 6.00 mmol) was added drop-wise. After 20 min of stirring at room temperature the reaction mixture was transferred to a separatory funnel, mixed with ether, and the organic layer was washed three times with a dilute potassium carbonate solution, and once with brine. The organic layer was dried with anhydrous magnesium sulfate, filtered and dried by rotary evaporation to yield the desired product (40-90% yield).

General procedure for preparation *tert*-butyl benzoylformates

5.00 mmol of a benzoylformic acid was combined with dichloromethane (3 mL) in a glass pressure bottle equipped with a magnetic stirring bar, and cooled in an acetone/dry ice bath. Sulfuric acid was added (28 µL) followed by liquid isobutylene (2-3 mL) and the bottle was sealed off. The reaction mixture was stirred at room temperature for 12 h. An excess of concentrated ammonia was added to neutralize the acid and the mixture was roto-evaporated to remove dichloromethane and unreacted isobutylene. Ether was added and washed three times with brine containing potassium carbonate. The ether layer was dried with anhydrous magnesium sulfate, filtered and rotary-evaporated to obtain the *tert*-butyl ester (40-60% yield).

^{1}H-NMR and Mass Spectrometry Data

^{1}H NMR spectra of MTh esters were obtained in MeOD-d_4 and referenced to the residual solvent C$\underline{H_3}$OH peak. The ^{1}H NMR spectrum of MTh was obtained in conc. DCl, and was referenced to the 3-(trimethylsilyl)-propionic 2,2,3,3-d_4 acid (TMSP-d_4) peak (0.00 ppm). ^{1}H NMR spectra of derivatives of MTh were obtained in 20% DCl and internally referenced to the C-6 pyrimidine peak at δ 6.86 ppm which was determined with MTh and TMSP-d_4 as standard.

_p_-OCH$_3$-MTh _tert_-butyl ester

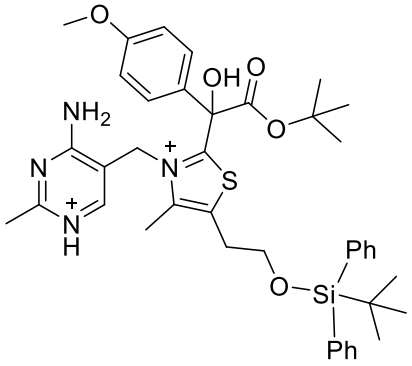

^{1}H NMR (300 MHz, MeOD-d_4) δ 7.65 (d, J = 7.7 Hz, 4H), 7.56 – 7.34 (m, 8H), 7.10 (s, 1H), 6.86 (d, J = 9.0 Hz, 0H), 5.72 (d, J = 17.7 Hz, 1H), 5.47 (d, J = 17.7 Hz, 1H), 3.97 (t, J = 5.4 Hz, 2H), 3.77 (s, 3H), 3.20

(t, *J* = 5.3 Hz, 2H), 2.51 (s, 3H), 2.32 (s, 3H), 1.48 (s, 9H), 1.07 (s, 9H). MS(ESI+) m/z: M^+ Calcd for $C_{41}H_{51}N_4O_5SSi^+$ 739.3 Found: 739.3

_p_-OCH_3-MTh

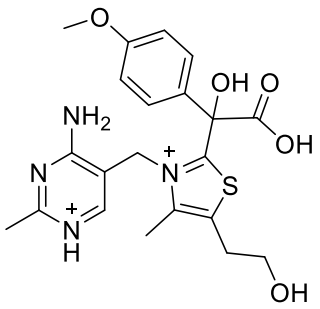

^{1}H NMR (300 MHz, 20% DCl) δ 7.52 (d, *J* = 8.9 Hz, 2H), 6.88 (apparent d, *J* = 8.9 Hz, 3H), 5.78 (d, *J* = 17.9 Hz, 10H), 5.43 (d, *J* = 17.9 Hz, 1H), 4.1 (t, *J* = 6.0 Hz, 2H), 3.81 (s, 3H), 3.29 (t, *J* = 6.0 Hz, 2H), 2.58 (s, 3H), 2.45 (s, 3H), MS(ESI+) m/z: M^+ Calcd for $C_{21}H_{25}N_4O_5S^+$ 445.15 Found: 401.2 [M - CO_2]

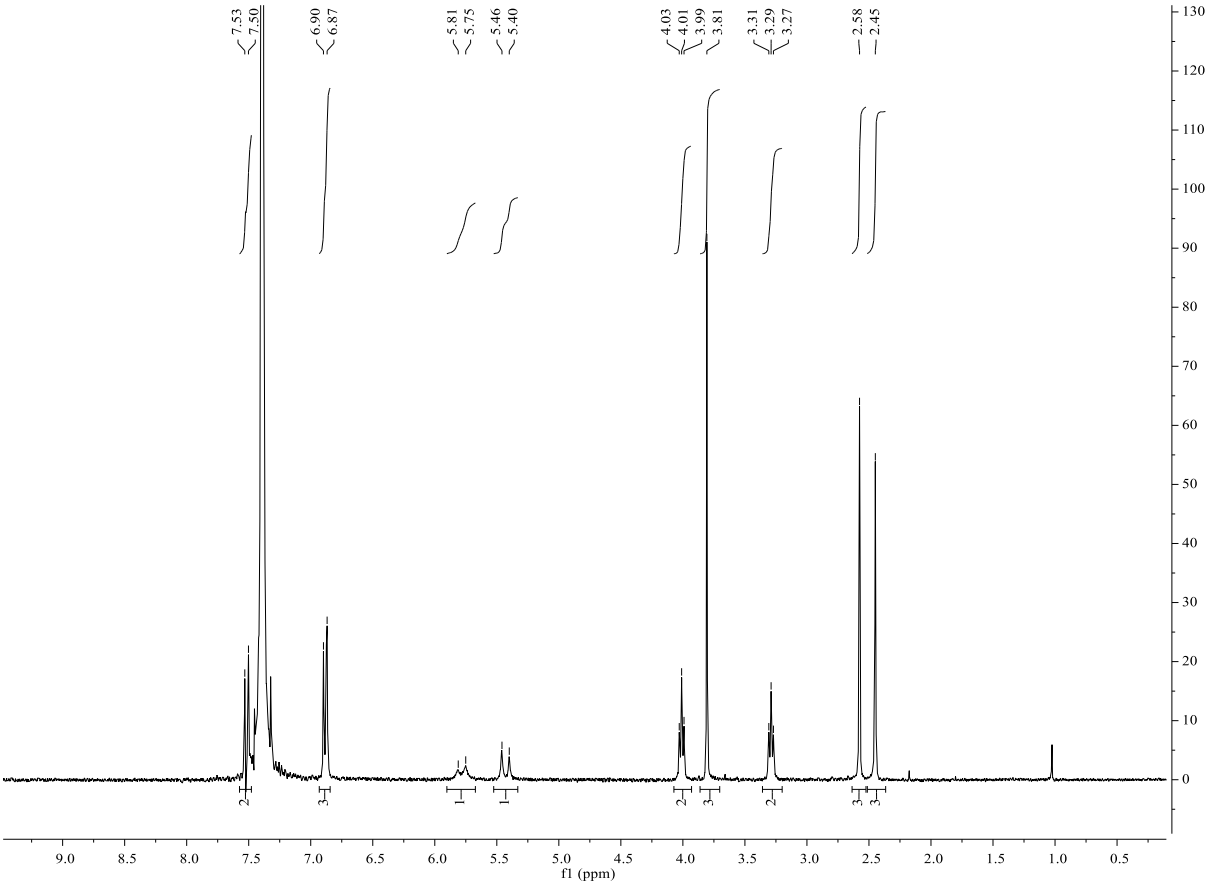

Figure S1. ^{1}H NMR (300 MHz, 20% DCl) spectrum of *p*-OCH_3 MTh derivative.

p-CH_3-MTh methyl ester

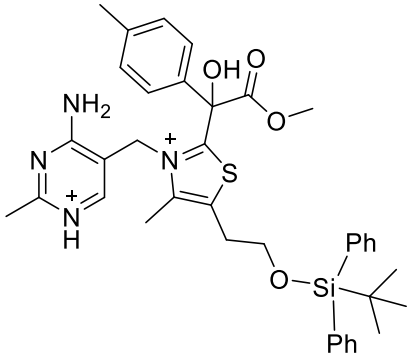

^{1}H NMR (300 MHz, MeOD-d_4) δ 7.69 – 7.61 (m, 4H), 7.51 – 7.38 (m, 8H), 7.23 – 7.15 (m, 3H), 5.68 (d, *J* = 17.4 Hz, 1H), 5.50 (d, *J* = 17.4 Hz, 1H), 3.97 (t, *J* = 5.4 Hz, 2H), 3.91 (s, 3H), 3.21 (t, *J* = 5.4 Hz, 2H), 2.54 (s, 3H), 2.34 (s, 3H), 2.28 (s, 3H), 1.05 (s, 9H). MS(ESI+) m/z: M^+ Calcd for $C_{38}H_{45}N_4O_4SSi^+$ 681.3 Found: 681.3

***p*-CH$_3$-MTh**

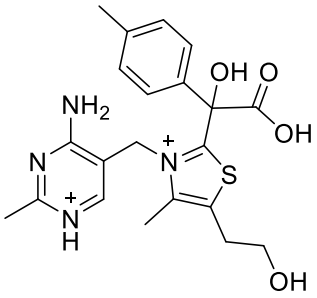

^{1}H NMR (300 MHz, 20% DCl) δ 7.47 (d, *J* = 8.2 Hz, overlap with H_2O peak), 7.18 (d, 2H), 6.86 (s, 1H), 5.83 (d, *J* = 18.4 Hz, 1H), 5.44 (d, *J* = 18.4 Hz, 1H), 4.03 (t, *J* = 5.7 Hz, 2H), 3.31 (t, *J* = 5.7 Hz, 2H), 2.62 (s, 1H), 2.46 (s, 1H), 2.25 (s, 1H). MS(ESI+) m/z: M^+ Calcd for $C_{21}H_{25}N_4O_4S^+$ 429.2 Found: 385.2 [M - CO_2]

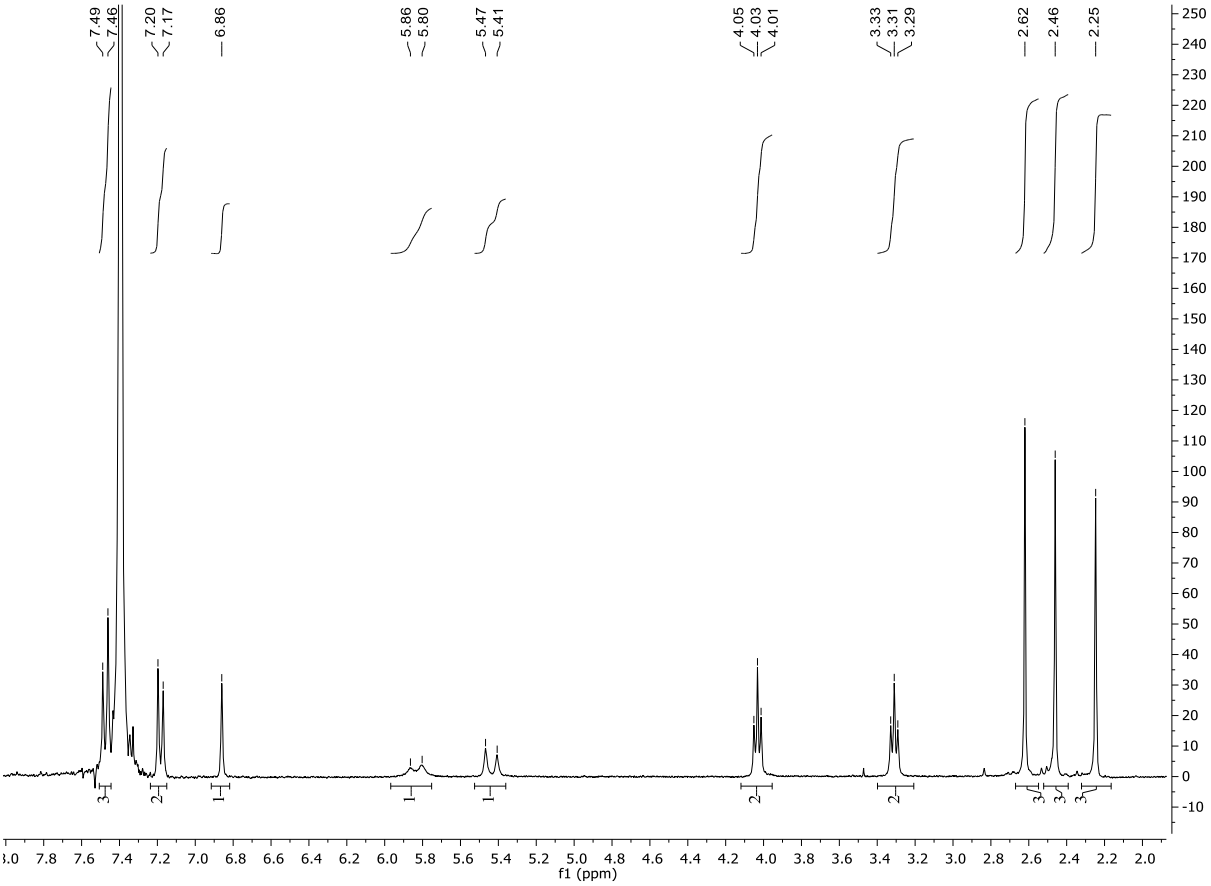

Figure S2. ^{1}H NMR (300 MHz, 20% DCl) spectrum of *p*-CH_3 MTh derivative.

MTh methyl ester

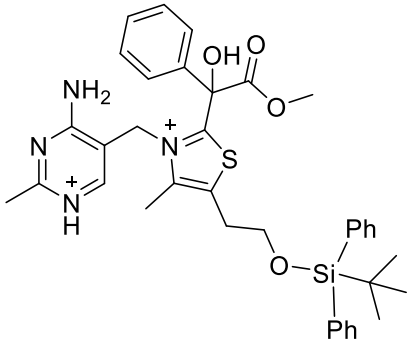

^{1}H NMR (600 MHz, MeOD) δ 7.65 (d, J = 7.8 Hz, 4H), 7.57 (d, J = 9.2 Hz, 2H), 7.51 – 7.38 (m, 9H), 7.20 (s, 1H), 5.70 (d, J = 17.6 Hz, 1H), 5.50 (d, J = 17.4 Hz, 1H), 3.97 (t, J = 5.4 Hz, 2H), 3.91 (s, 3H), 3.21 (t, J = 5.4 Hz, 2H), 2.52 (s, 3H), 2.34 (s, 3H), 1.06 (s, 9H). MS(ESI+) m/z: M^+ Calcd for $C_{37}H_{43}N_4O_4SSi^+$ 667.3 Found: 667.3

MTh

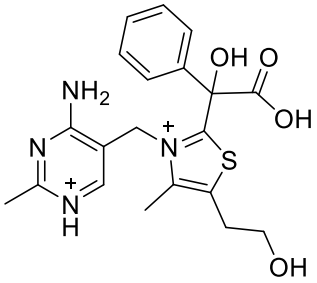

^{1}H NMR (400 MHz, 20% DCl, TMSP-d_4) δ 7.59 – 7.54 (m, 2H), 7.35 – 7.26 (m, 3H), 6.86 (s, 1H), 5.82 (d, *J* = 19.5 Hz, 1H), 5.40 (d, *J* = 19.5 Hz, 1H), 3.98 (t, *J* = 5.7 Hz, 2H), 3.26 (t, *J* = 5.7 Hz, 2H), 2.54 (s, 3H), 2.41 (s3H). MS(ESI+) m/z: M^+ Calcd for $C_{20}H_{23}N_4O_4S^+$ 415.1 Found: 371.1 [M - CO_2]

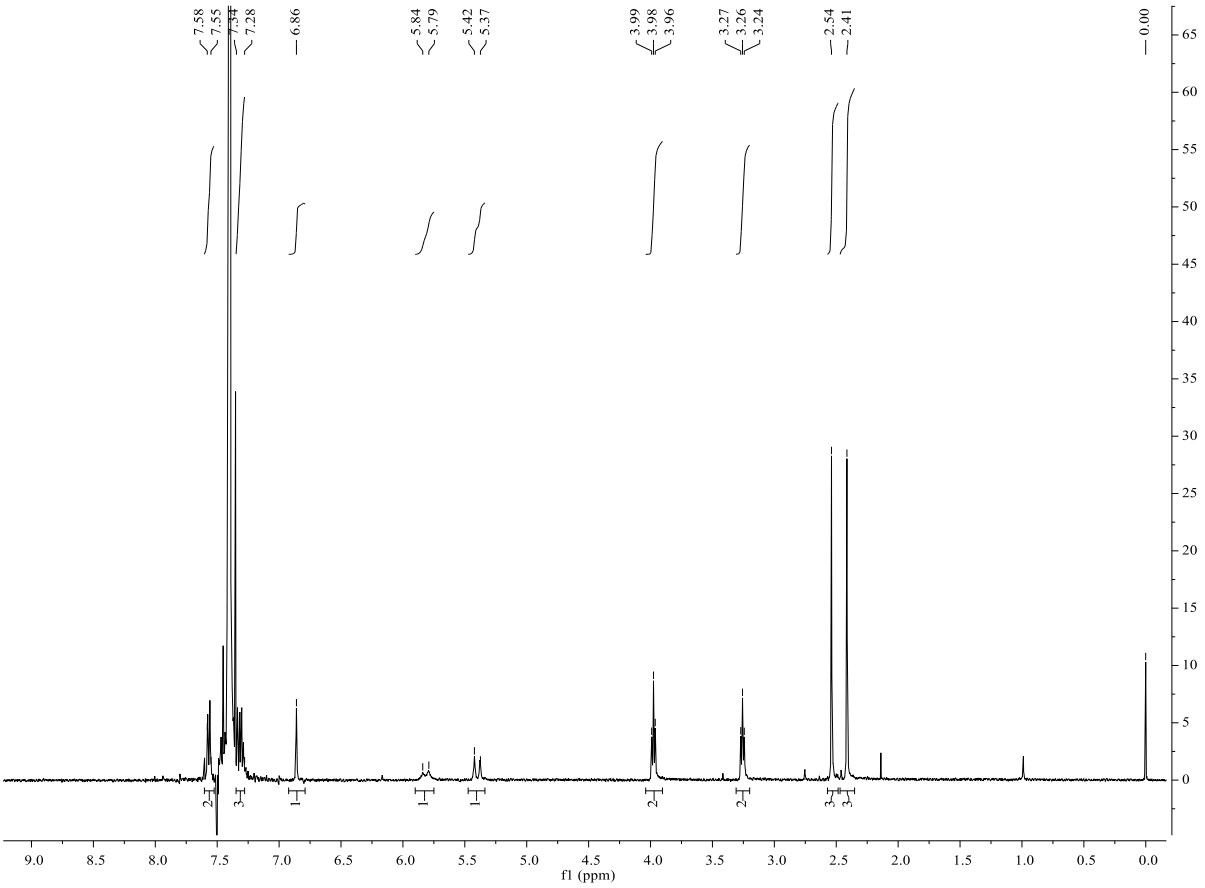

Figure S3. ^{1}H NMR (400 MHz, 20% DCl, TMSP-d_4) spectrum of MTh.

p-F-MTh methyl ester

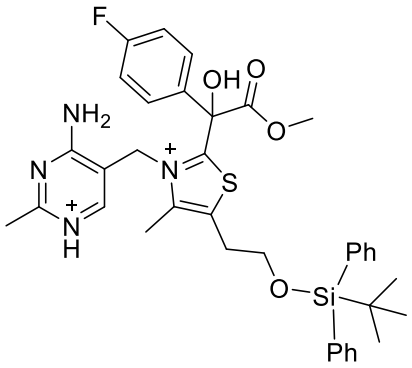

^{1}H NMR (300 MHz, MeOD-d_4) δ 7.74 – 7.58 (m, 6H), 7.49 – 7.37 (m, 7H), 7.13 (t, J = 8.7 Hz, 2H), 5.69 (d, J = 17.5 Hz, 1H), 5.53 (d, J = 17.5 Hz, 1H), 3.98 (t, J = 5.4 Hz, 2H), 3.91 (s, 3H), 3.22 (t, J = 5.4 Hz, 2H), 2.55 (s, 3H), 2.37 (s, 3H), 1.05 (s, 9H). MS(ESI+) m/z: M^+ Calcd for $C_{37}H_{43}FN_4O_4SSi^+$ 685.3 Found: 685.3

***p*-F-MTh**

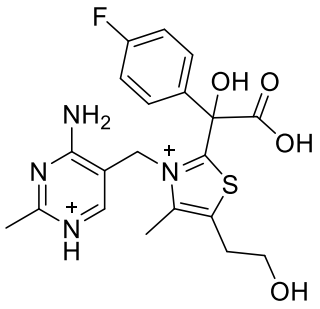

^{1}H NMR (300 MHz, 20% DCl) δ 7.46 (dd, *J* = 9.0, 5.1 Hz, 2H), 6.96 (t, *J* = 8.8 Hz, 2H), 6.86 (s, 1H), 5.63 (d, *J* = 18.0 Hz, 1H), 5.27 (d, *J* = 18.0 Hz, 1H), 3.81 (t, *J* = 5.8 Hz, 2H), 3.10 (t, *J* = 5.7 Hz, 2H), 2.42 (s, 3H), 2.28 (s, 3H). MS(ESI+) m/z: M^+ Calcd for $C_{20}H_{22}FN_4O_4S^+$ 433.1 Found: 389.1 [M - CO_2]

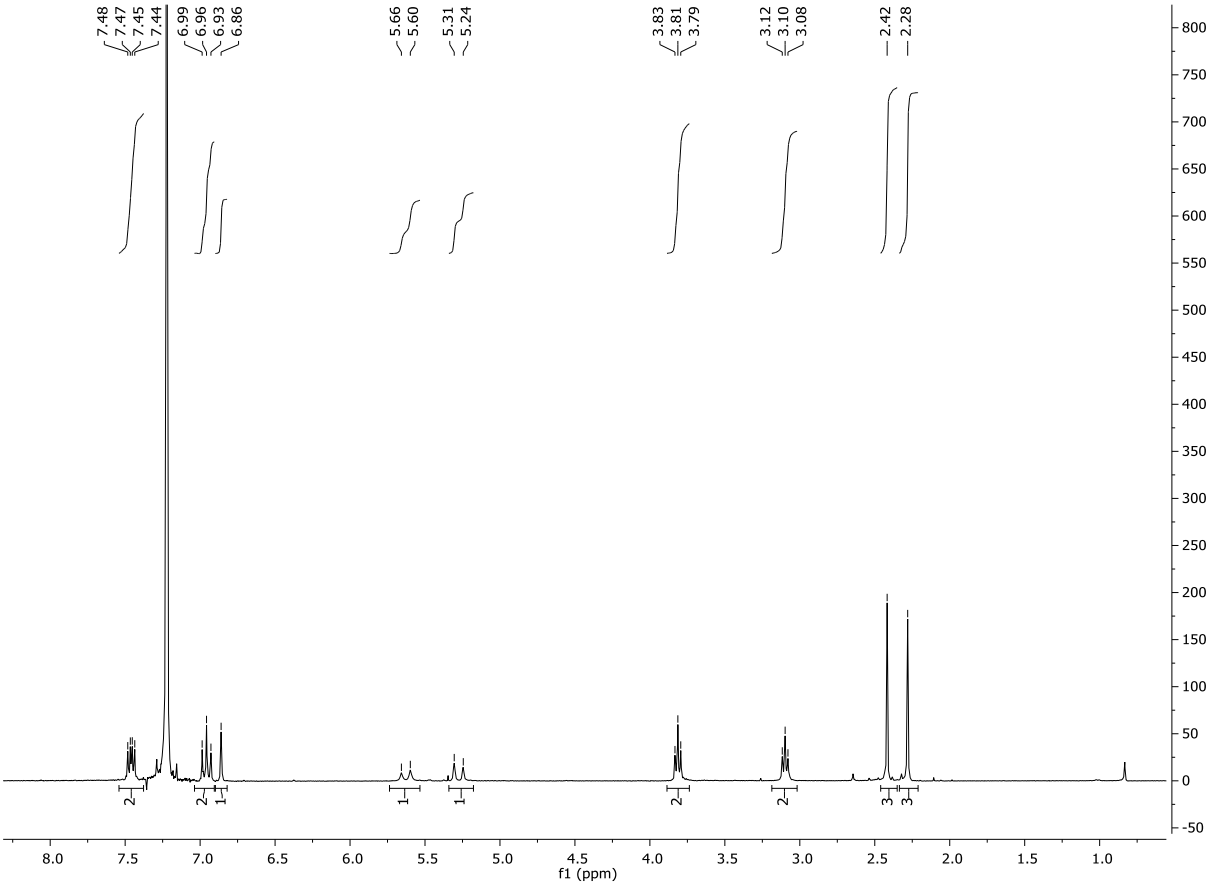

Figure S4. ^{1}H NMR (300 MHz, 20% DCl) spectrum of *p*-F MTh derivative.

***p*-Cl-MTh methyl ester**

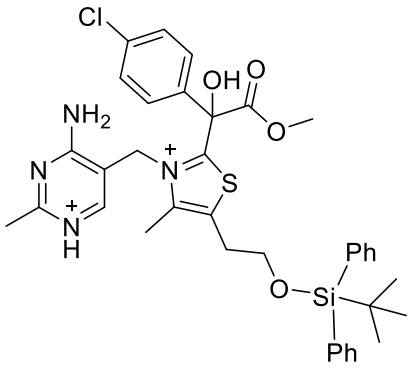

^{1}H NMR (300 MHz, MeOD-d_4) δ 7.68-7.65 (m, 4H), 7.58 – 7.35 (m, 11H), 7.26 (s, 1H), 5.73 (d, *J* = 18.0 Hz, 1H), 5.47 (d, *J* = 18.0 Hz, 1H), 3.98 (t, *J* = 5.4 Hz, 2H), 3.91 (s, 3H), 3.22 (t, *J* = 5.4 Hz, 2H), 2.56 (s, 3H), 2.35 (s, 3H), 1.07 (s, 9H). MS(ESI+) m/z: M^+ Calcd for $C_{37}H_{42}ClN_4O_4SSi^+$ 701.2 Found: 701.2

***p*-Cl-MTh**

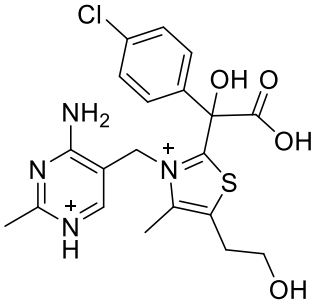

^{1}H NMR (300 MHz, 20% DCl) δ 7.51 (d, *J* = 8.8 Hz, 2H), 7.29 (d, *J* = 8.8 Hz, 2H), 6.86 (s, 1H), 5.79 (d, *J* = 18.4 Hz, 1H), 5.33 (d, *J* = 18.4 Hz, 1H), 3.94 (t, *J* = 5.8 Hz, 2H), 3.22 (t, *J* = 5.8 Hz, 2H), 2.57 (s, 3H), 2.38 (s, 3H). MS(ESI+) m/z: M^+ Calcd for $C_{20}H_{22}ClN_4O_4S^+$ 449.1 Found: 405.1 [M - CO_2]

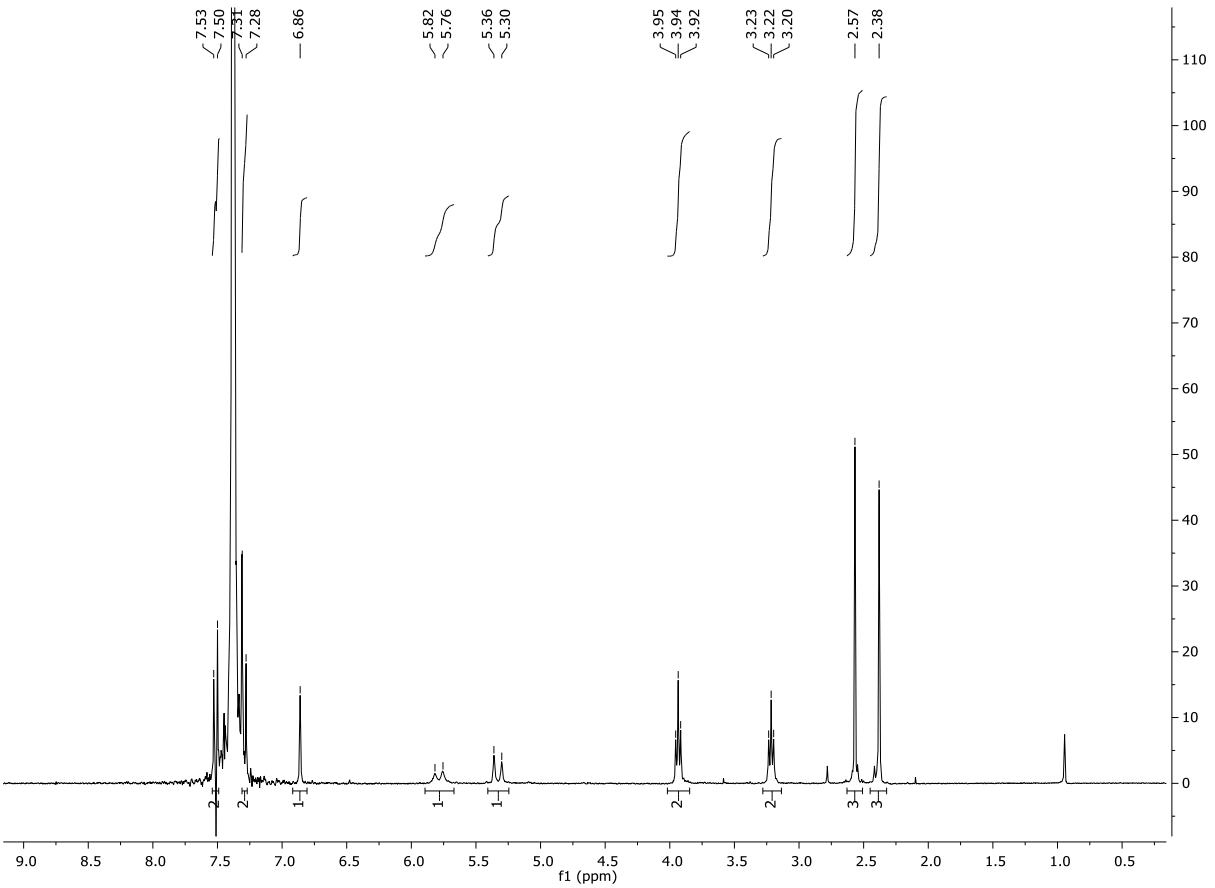

Figure S5. [1]H NMR (300 MHz, 20% DCl) spectrum of *p*-Cl MTh derivative.

m-Br-MTh methyl ester

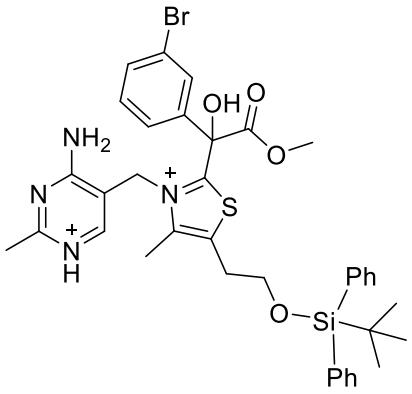

[1]H NMR (600 MHz, MeOD) δ 7.76 (t, *J* = 1.8 Hz, 1H), 7.69 – 7.62 (m, 4H), 7.53 (ddd, *J* = 8.0, 1.9, 0.9 Hz, 1H), 7.52 – 7.47 (m, 3H), 7.47 – 7.42 (m, 4H), 7.29 (t, *J* = 8.0 Hz, 1H), 7.25 (s, 1H), 5.72 (d, *J* = 17.5 Hz, 1H), 5.47 (d, *J* = 17.5 Hz, 1H), 3.98 (t, *J* = 5.4 Hz, 2H), 3.91 (s, 3H), 3.22 (t, *J* = 5.4 Hz, 2H), 2.54 (s, 3H), 2.35 (s, 3H), 1.07 (s, 9H). MS(ESI+) m/z: M^+ Calcd for $C_{37}H_{42}BrN_4O_4SSi^+$ 745.2 Found: 745.2

***m*-Br-MTh**

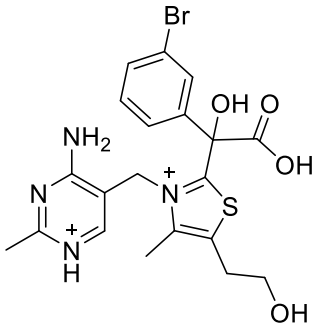

^{1}H NMR (400 MHz, 20% DCl) δ 7.63 (s, 1H), 7.41 (d, *J* = 8.0 Hz, 1H), 7.31 (d, *J* = 8.0 Hz, 1H), 7.12 7.07 (t, *J* = 8.0 Hz, 1H), 6.86 (s, 1H), 5.73 (d, *J* = 19.2 Hz, 1H), 5.27 (d, *J* = 18.0 Hz, 1H), 3.86 (t, *J* = 5.6 Hz, 4H), 3.15 (t, *J* = 5.6 Hz, 2H), 2.44 (s, 2H), 2.32 (s, 2H). MS(ESI+) m/z: M^+ Calcd for $C_{20}H_{22}BrN_4O_4S^+$ 493.1 Found: 449.1 [M - CO_2]

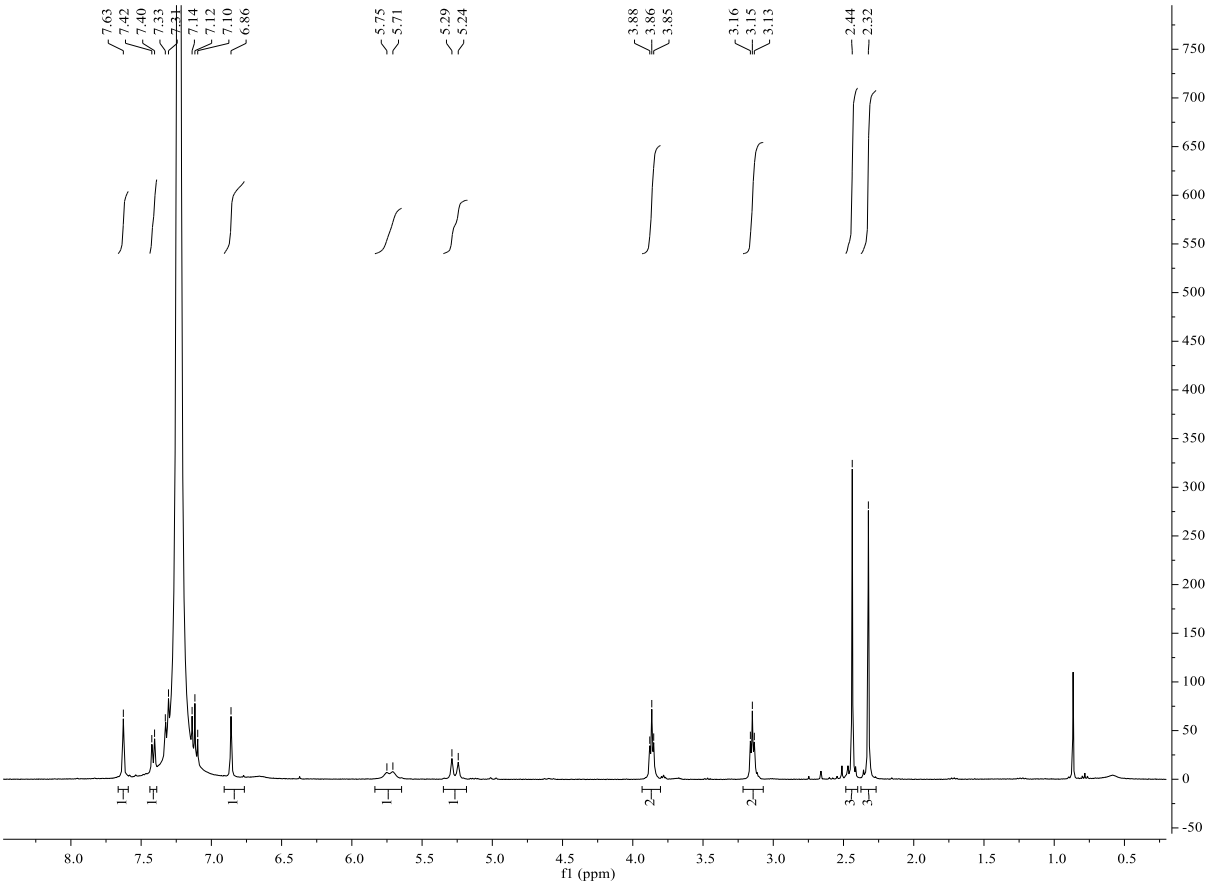

Figure S6. ^{1}H NMR (300 MHz, 20% DCl) spectrum of *m*-Br MTh derivative.

Kinetics

The decarboxylation of the various MTh derivatives was conducted in pH 7.0 HEPES buffers (0.100, 0.200, 0.300 and 0.400 M) and ionic strength equal to 1.000 M (KCl). The progress of the reaction was followed by UV-VIS spectroscopy at 25.0(±0.1) ^{o}C. All decarboxylation reactions showed perfect 1st order kinetics which was evident in sharp isosbestic points and very good exponential fits. Observable rate constants were calculated from exponential fits (GraFit) at 328 nm, where the change in absorbance was the largest. These values were essentially identical to the ones obtained at 290 nm. The 328 nm absorbance is a result of a very fast (10^{4} s^{-1}) fragmentation reaction, occurring from the post-decarboxylation intermediate (Breslow intermediate). The resulting benzoylthiazole (PTK) derivative has a red-shifted absorbance because of the extended conjugation. The decarboxylation step is relatively slow (~10^{-4} s^{-1}), and the rate for formation of the PTK derivative is representative of the rate-limiting decarboxylation step. All measurements were done in triplicates. All reported rate constants are for zero buffer concentration, and were obtained by a linear

extrapolation in the buffer concentration plots. Product study by ^{1}H NMR revealed the formation of both the protonation and fragmentation products, consistent with previous reports.

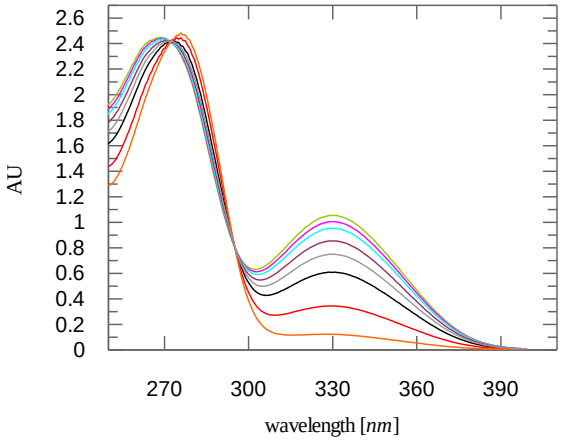

Figure S7. An example of a typical UV-VIS spectroscopy time-study of the decarboxylation of a MTh derivative in a pH 7.0 buffer. The increase at 328 nm is the result of a very fast (~10^4 s^{-1}) fragmentation reaction, resulting in formation a PTK derivative.

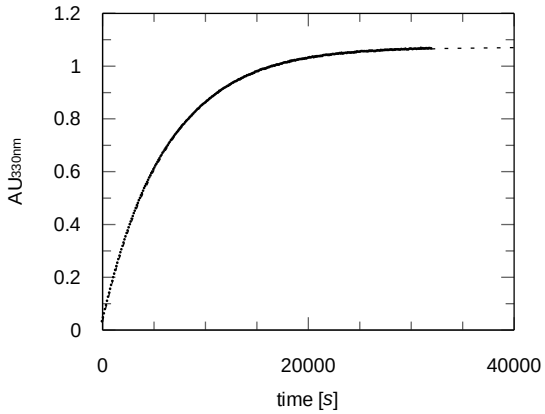

Figure S8. An example of a 328 nm absorbance change as the decarboxylation reaction progresses with time.

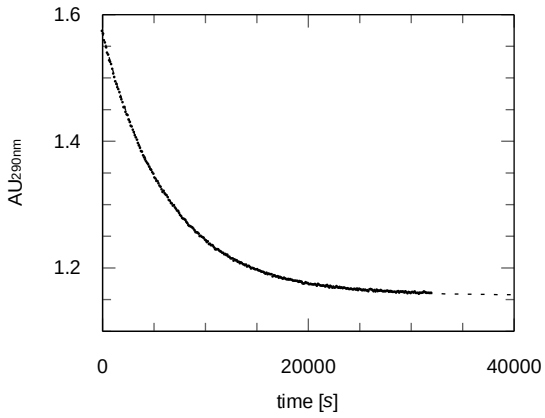

Figure S9. An example of 290 nm absorbance change as the decarboxylation reaction progresses with time.

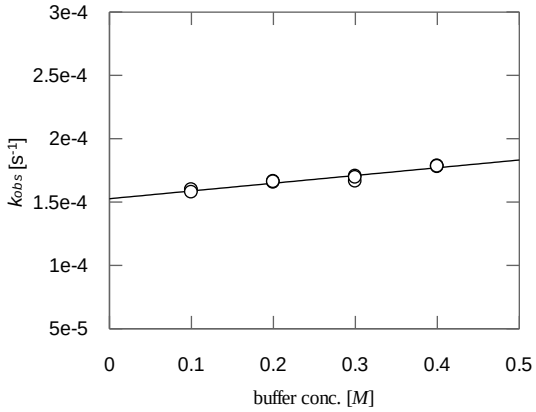

Figure S10. A representation of a typical buffer dependency plot for the decarboxylation of a MTh derivative.

Table S1. Rate constants (*k*) for the decarboxylation of MTh and derivatives at pH = 7.0 in water at 25.0(±0.1) ºC. The corresponding Hammett sigma values (σ) are also shown.

Z	σ	$10^{-4}\times k$ s^{-1}
p-MeO	-0.27	1.53(±0.05)
p-Me	-0.17	1.52(±0.05)
H	0	2.15(±0.05)
p-F	0.06	2.80(±0.06)
p-Cl	0.23	2.30(±0.07)
m-Br	0.39	0.39(±0.05)

References

(1) Zhuang, J.; Wang, C.; Xie, F.; Zhang, W. (2009) One-pot efficient synthesis of aryl α-keto esters from aryl-ketones, *Tetrahedron. 65*, 9797-9800.

(2) Bielecki, M.; Kluger, R. (2017) The need for an alternative to radicals as the cause of fragmentation of a thiamin-derived breslow intermediate, *Angew. Chem., Int. Ed. Engl. 56,* 6321-6323.